Supplementary information for: Flow-driven pattern formation during coacervation of xanthan gum with a cationic surfactant

Yorgos Stergiou,[1,2,*] Alexandros Perrakis,[1,2]
Anne De Wit,[3] and Karin Schwarzenberger[1,2,†]

[1] *Institute of Fluid Dynamics, Helmholtz-Zentrum Dresden-Rossendorf, Bautzner Landstr. 400, 01328 Dresden, Germany*

[2] *Institute of Process Engineering and Environmental Technology, Technische Universität Dresden, 01062 Dresden, Germany*

[3] *Nonlinear Physical Chemistry Unit, Service de Chimie Physique et Biologie Théorique, Faculté des Sciences, Université Libre de Bruxelles (ULB), CP 231, 1050 Brussels, Belgium*

In Table S1, the experimental parameters (gap height, h, and flow rate, q) along with their calculated Ra and Pe values are presented. 2-5 repetitive runs are performed for each value of parameters.

TABLE S1: List of experiments

Gap height, h (mm)	Flow rate, q (ml/min)	Pe	Ra
0.1	0.005	1 326	876
0.1	0.01	2 652	876
0.1	0.012	3 183	876
0.1	0.013	3 448	876
0.1	0.015	3 979	876
0.1	0.02	5 305	876
0.1	0.12	31 830	876
0.1	0.4	106 099	876
0.1	0.5	132 624	876
0.25	0.02	2 122	13 693
0.25	0.1	10 610	13 693
0.25	0.2	21 220	13 693
0.25	0.5	53 050	13 693
0.5	0.1	5 305	109 544
0.5	0.5	26 525	109 544
0.5	1	53 050	109 544
0.6	0.08	3 537	189 292
0.6	0.3	13 262	189 292
0.6	0.4	17 683	189 292

* g.stergiou@hzdr.de
† k.schwarzenberger@hzdr.de

TABLE S1: List of experiments (continued)

Gap height, h (mm)	Flow rate, q (ml/min)	Pe	Ra
0.6	0.5	22 104	189 292
0.6	0.7	30 946	189 292
0.6	0.8	35 366	189 292
0.6	1	44 208	189 292
0.6	2	88 416	189 292
0.75	0.08	2 829	369 711
0.75	0.1	3 537	369 711
0.75	0.5	17 683	369 711
0.75	1	35 366	369 711

In Figure S1, the temporal evolution of the pattern outline is depicted for the viscous fingering (VF) regime (a), the "fan" regime (b) and the "volcano" regime (c). The early stages are represented by darker, the later stages by brighter colors. The VF outlines have a roughly spherical shape, while the patterns in the fan regime become asymmetrical. The volcano regime is characterized by an irregular and strongly localized growth.

Despite the asymmetry in the fan regime, the pattern still grows steadily while the progression is highly intermittent in the volcano regime. This is caused by the buoyancy-induced layering of the coacervate in the volcano regime and the resulting 3D pattern structure. Two area growth curves, i.e. $\mathrm{d}A/\mathrm{d}t$, are shown in Figure S2. The steady growth due to the gap-spanning coacervate front in the fan regime is characterized by a rather smooth curve progression in Figure S2(a). The large fluctuations in the volcano regime in Figure S2(b) indicate the 3D growth of the coacervate pattern, where only the growth in the horizontal direction can be visualized

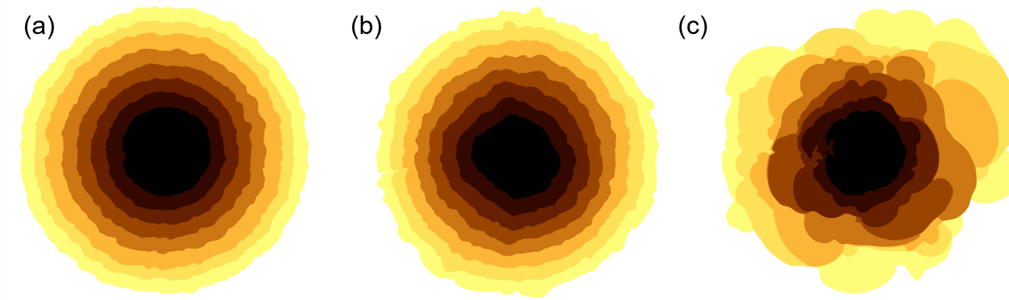

FIG. S1. Temporal evolution of pattern outline in the viscous fingering (a); fan (b) and volcano regime (c). The shown cases are for Pe = 53 050, Ra = 109 544 (a), Pe = 26 525, Ra = 109 544 (b) and Pe = 3 537, Ra = 369 711 (c).

properly and the growth in the vertical direction is partly covered by the already existing coacervate layers.

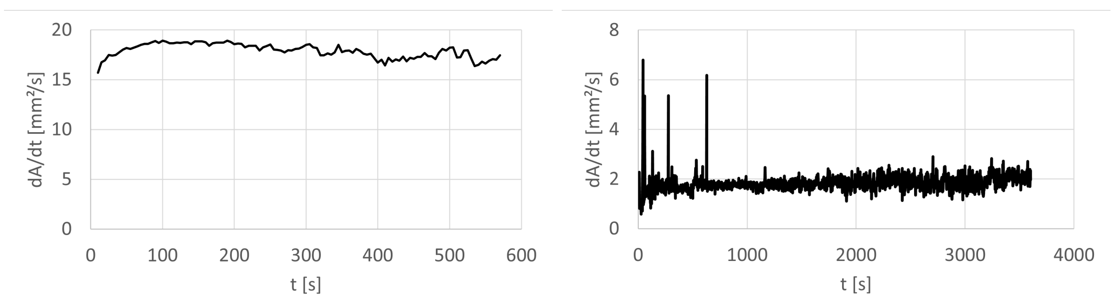

(a) (b)

FIG. S2. Temporal change of the area of the pattern, dA/dt, in the fan (a) and volcano regime (b). The shown cases are for Pe = 26 525, Ra = 109 544 (a) and Pe = 3 537, Ra = 369 711 (b).

Figure S3(a,b) shows a weak buoyancy-driven instability for a large gap width in the non-reactive case due to the density difference between both fluids. No pronounced structures are observed in the early stages of the displacement, while the strongly asymmetric bulging in the volcano regime is present already at the beginning. Indeed, the fingering zone in the coacervation system rather reduces with time, whereas the slight buoyancy-driven modulations in the non-reactive displacement become only visible after a distinct onset time. For the small gap width in Figure S3(c,d), the instability is absent throughout the whole experiment.

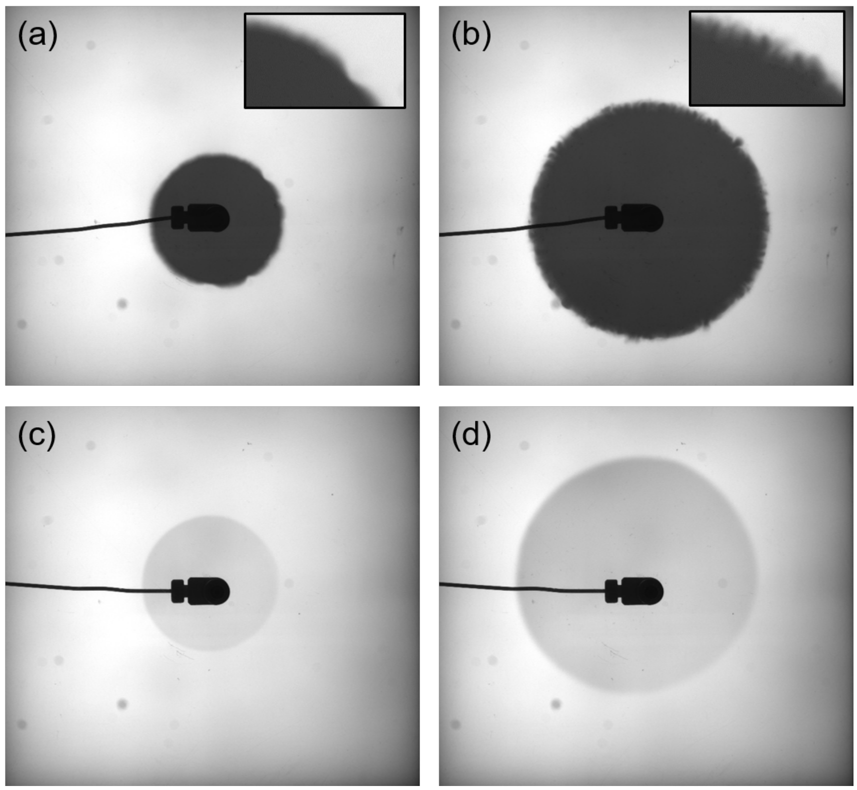

FIG. S3. Snapshots for the non-reactive injection of the xanthan gum dispersion (higher density) into pure water (lower density). For a large gap width (h = 0.5 mm, flowrate q = 0.1 ml/min) a slight buoyancy-driven instability develops with time (a,b). The inset shows a detail of the weak modulations of the XG front due to the emerging instability. For a small gap width (h = 0.1 mm, flowrate q = 0.012 ml/min) any pattern formation is absent (c,d).